

Nucleation and growth of self-assembled Ge/Si(001) quantum dots

Vinh Le Thanh, P. Boucaud, and D. Débarre

Institut d'Electronique Fondamentale, URA-CNRS 22, Bâtiment 220, Université Paris-Sud, 91405 Orsay, France

Y. Zheng

Laboratoire Minéralogie-Cristallographie, URA-CNRS 09, Université Paris VI, 4 Place Jussieu, 75252 Paris Cedex 5, France

D. Bouchier and J.-M. Lourtioz

Institut d'Electronique Fondamentale, URA-CNRS 22, Bâtiment 220, Université Paris-Sud, 91405 Orsay, France

(Received 14 April 1998; revised manuscript received 27 July 1998)

In situ reflection high-energy electron diffraction along with atomic-force microscopy and photoluminescence spectroscopy have been used to investigate the Ge/Si(001) growth process in an ultrahigh-vacuum chemical-vapor-deposition system at temperatures varying from 550 to 700 °C. The existence of an intermediate phase between *entirely pseudomorphic two-dimensional (2D)* layers and *3D macroscopic islands* is established. This phase which consists of pyramidal clusters with a squared base and {105} facets is found to be metastable with regard to the formation of 3D macroscopic islands. Two kinetic pathways for the growth of 3D macroscopic islands are identified versus growth temperature. At 550 °C the growth proceeds near equilibrium configuration and islands of monosize distribution can be formed. At 700 °C, coalescence is found to take place even at the early stage of growth, which results in the formation of highly inhomogeneous islands. [S0163-1829(98)03443-2]

During the past few years, a considerable amount of work has been devoted to the formation of quantum dots (QD's) due to their potential interest for electronic and optoelectronic device applications.¹ Among the different ways to produce QD's, special attention has been paid to the self-assembled technique, which takes advantage of the transition from the two-dimensional (2D) to 3D growth mode occurring during growth in a highly lattice-mismatched heteroepitaxial system.² Using this approach, it has been shown that islands with sizes in the quantum range (~30 nm) could be achieved in III-V materials.³ Concerning the Ge/Si system, islands with large sizes (>100 nm) and broad size distributions (>10%) were generally reported.^{4,5}

Molecular-beam epitaxy (MBE), including gas-source MBE and chemical-vapor deposition (CVD) are the two main techniques that are used to grow Ge/Si QD's. In MBE or GS-MBE growth, thanks to the capability of a monolayer-scale control of the growth rate and of real-time and *in situ* monitoring of the growing surface by powerful surface-sensitive techniques such as reflection high-energy electron diffraction (RHEED) and scanning tunneling microscopy, a relatively detailed picture of the island morphological evolution has been obtained.⁶⁻⁸ One of the most significant results is the discovery of an *intermediate* 3D phase consisting of elongated and hutlike-shaped clusters formed by {501} facets (referred to as "hut" clusters).⁶ These clusters have since been identified by different structural characterizations, but to our knowledge, their optical properties have not been reported yet. Note that the metastability of this cluster phase has not been clearly demonstrated: for instance, the coexistence of the hut clusters and 3D macroscopic islands as indicated in Fig. 1(b) of Ref. 6 would suggest that the hut clusters are not metastable.

The kinetics of island growth using CVD instead of MBE are not fully understood. This is in part due to the variety and complexity of the processes involved in the CVD growth.⁹ Besides, the very high pressures used during growth limit the use of conventional surface techniques to characterize the growth processes. Some of the previous studies have, for example, investigated the evolution of the surface morphology as a function of the deposition time^{5,10,11} but the 2D-3D transition, which is crucial for controlling the island distribution, was not precisely identified.

In this work, we use *in situ* RHEED to monitor in real time the Ge/Si(100) growth processes in an ultrahigh-vacuum (UHV)-CVD system. Our RHEED gun is equipped with a differential pumping option, allowing us to probe the growing surface even at high partial pressures of hydrides (up to 10⁻¹ Torr). At each growth step identified by RHEED, structural characterizations by atomic-force microscopy (AFM) along with optical characterizations performed with photoluminescence (PL) were combined to investigate the island formation.

Experiments were carried out in a MBE system that has been modified to accommodate hydride sources and RHEED setup. Pure SiH₄ and hydrogen-diluted (10%) GeH₄ were used as gas sources. The system has a base pressure better than 1 × 10⁻¹⁰ Torr, and the pressure during growth was about 5 × 10⁻³ Torr. Details of the experimental setup and growth conditions have been reported elsewhere.¹² The sample temperature was measured with an IR pyrometer (Irron, W series), the accuracy of the temperature measurement being of about ±10 °C. The thickness of the Ge films were estimated by high-resolution transmission electron microscopy (HRTEM) with an accuracy of about 20%. The sizes and the density of islands were measured with a Park Scientific Instruments AFM operating in a contact mode. The pho-

toluminescence was excited with an argon ion laser and detected with a liquid-nitrogen-cooled Ge photodetector using standard lock-in techniques.

Ge deposition was investigated at temperatures between 550 and 700 °C. At each growth temperature, two series of samples were grown. Reference samples without a Si cap were prepared for AFM analysis. A second series of samples with a 30-nm-thick Si cap layer on top of the Ge layer was grown for PL measurements. We present here results at two typical temperatures, 550 and 700 °C. A complete analysis in the whole temperature range of investigation will be presented elsewhere.

It is now well established that the Ge/Si growth follows a Stranski-Krastanow growth mode, the 2D-3D growth mode transition being easily detected by RHEED. The 2D growth regime is associated with the observation of streaky patterns, while the 3D growth is characterized by spotty patterns due to transmission diffraction through 3D islands.¹³ The 2D-3D transition is known to be sharp, allowing a relatively precise determination of the wetting layer thickness or the deposition time at which 3D growth occurs.¹⁴ During our experiments, RHEED patterns were recorded using a camera-based video recording system. The 2D-3D transition determined from RHEED occurred after 150 s for a deposition carried out at 700 °C and 240 s for a deposition at 550 °C. The corresponding thickness of the wetting layers, estimated from HRTEM, was ~ 3 and in between 3 and 4 ML, respectively. However, looking at the RHEED patterns just before the 2D-3D transition, even though a streaky pattern characteristic of a 2D growth was present, a pronounced reinforcement of the intensity of 1×1 streaks was observed while the intensity of $\frac{1}{2}$ streaks considerably decreased. What was more intriguing was the growth behavior of the Si capping layers. Three distinct behaviors were observed depending on the morphology of the Ge surface. When starting from the wetting layer Ge surface characterized by a well-developed streaky pattern, no change in RHEED patterns was detected during all the Si deposition process, indicating that the buried Ge layers were entirely pseudomorphic. If Si was deposited on the Ge surface after the stage of 3D island formation, the deposited Si was found to progressively smooth the surface. However, if Si was deposited on the Ge surface just before the 2D-3D transition, islands started to grow for the first Si layers and then a progressive smoothening of the surface took place. These observations thus prompted us to undertake systematic AFM and PL studies close to the 2D-3D transition. We note that this behavior was observed over the whole temperature range under investigation.

Figure 1 shows the evolution of the PL spectrum of a Ge layer grown at 700 °C with the deposition times (t_g). We recall that the 2D-3D transition determined from RHEED occurs at $t_g = 150$ s. Apart from the narrow peak at 1100 meV that is attributed to the phonon-assisted recombination of the free-exciton in the silicon substrate, the spectra of samples grown for 40 and 70 s are dominated by two main lines. They are attributed to the excitonic no-phonon (NP) and transverse-optical (TO)-phonon-assisted transitions of pseudomorphic Ge layers in Si.¹⁵ The energy difference between the NP and TO lines is ~ 58 meV. The shift of these two lines towards lower energies when the deposition time increases from 40 to 70 s can be explained by the decrease of

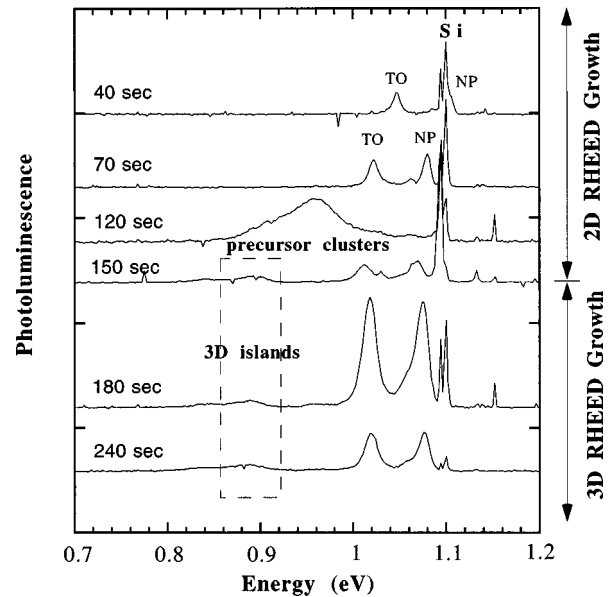


FIG. 1. 5-K PL spectra of a Ge layer grown at 700 °C with various deposition times. The 2D-3D transition determined from RHEED occurs at 150 s. We note that the 120-s sample spectrum obtained just before the 2D-3D transition detected by RHEED is dominated by an intense and very broad band centered at ~ 960 meV while the two NP and TO lines characteristic of the wetting layer have almost disappeared. This band completely disappears for sample growths larger than 150 s, i.e., after the formation of 3D macroscopic islands.

the confinement energy along the growth direction with increasing the thickness of the wetting layer. For samples obtained after the 2D-3D transition (150, 180, and 240 s), the spectra reveal a new luminescence band, apart from the NP and TO lines. The latter which is maximum at ~ 890 meV can be attributed to 3D macroscopic islands (MI's). We note that the energy maximum of this band does not shift in energy for growth times up to 240 s. These observations are expected and support in some way previous studies.^{16,17} The major new feature of our results concerns the 120-s sample spectrum obtained just before the 2D-3D transition detected by RHEED. The spectrum is dominated by an intense and very broadened band centered at ~ 960 meV while the two NP and TO peaks characteristic of the wetting layer have almost disappeared. The higher energy of this band compared to that of 3D MI's indicates that the corresponding islands have smaller sizes than the 3D ones. The broadening in energy (~ 100 meV) reflects, on the other hand, a large size distribution of islands. Note that this band appears on a very short interval of growth time. It completely disappears after the formation of 3D MI's, i.e., for sample growths larger than 150 s.

The surface morphology state at this growth stage ($t_g = 120$ s) is presented in Fig. 2. Whereas for shorter deposition times the surface is planar, the present surface exhibits islands with a very low density, near $6 \times 10^7 \text{ cm}^{-2}$. The islands have a height of ~ 1 – 2 nm while their widths vary from 32 to 46 nm [see the size histogram in Fig. 2(b)]. This broad dispersion in size confirms the broadening observed in PL. Displayed in the inset is an image of a single island. The island exhibits a truncated pyramidal shape with four side-

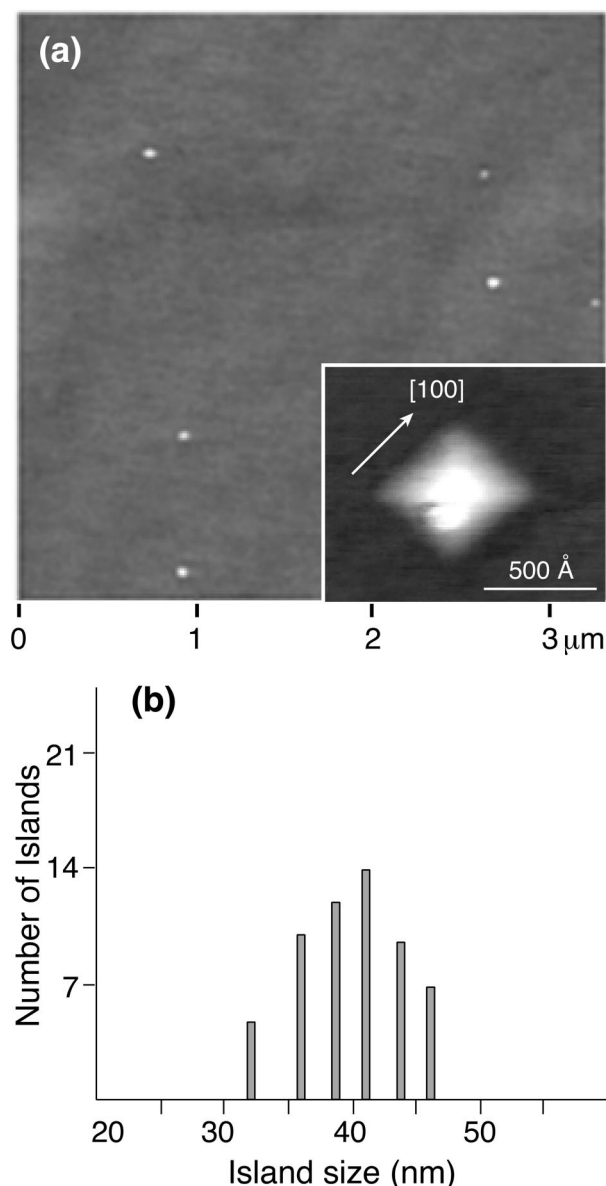


FIG. 2. AFM images of the 120-s sample grown at 700 °C. Shown in the inset is an image of a single island. The island is a truncated pyramid formed by four $\{105\}$ facets on a squared base and terminated at the top by a $\{100\}$ plane. (b) A histogram of island size distributions obtained from eight AFM images with scan size of $3.3 \times 3.3 \mu\text{m}$.

wall facets formed by $\{105\}$ planes (the mean inclination angles determined from AFM cross sectional height profiles of islands is $\sim 11^\circ$) and terminated on the top by a $\{100\}$ plane. Unlike the “hut” clusters observed in MBE growth,⁶ the islands presently observed have a much lower concentration and lie on a squared base instead of the elongated base of the hut clusters.

Figure 3 shows an AFM image of the surface just after the appearance of 3D spots in RHEED patterns ($t_g = 150$ s). The size distribution is presented in Fig. 3(b). It is clearly seen that the pyramidal islands described above have completely disappeared. The surface is now characterized by two kinds of islands exhibiting a “dome” shape with larger angle facets. A similar bimodal distribution has already been reported in the literature.^{11,18} The small islands (indicated by A)

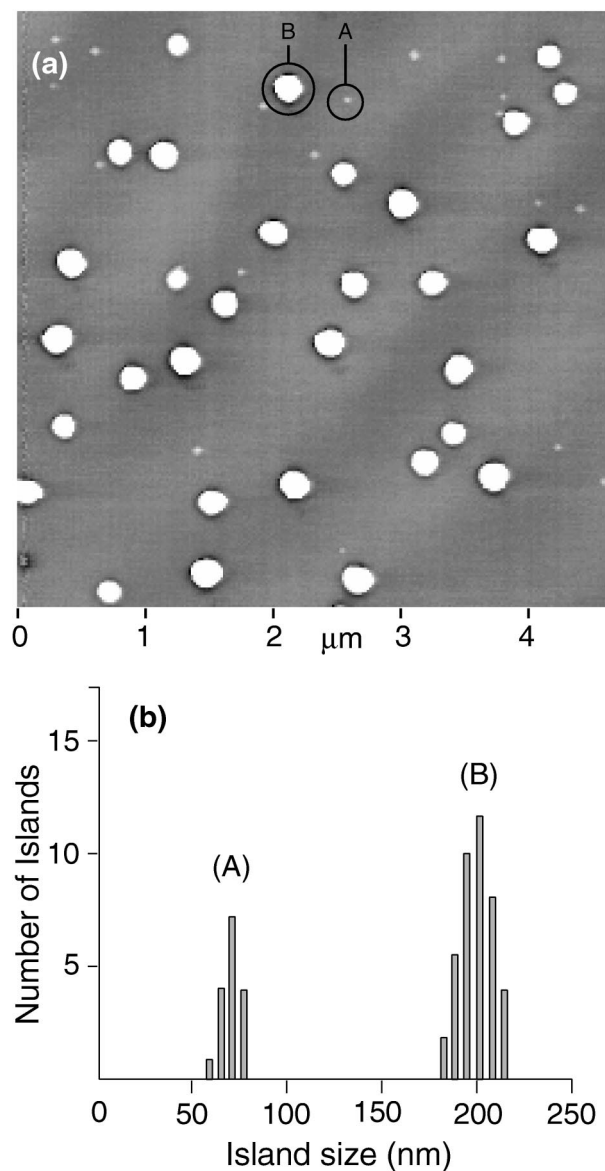


FIG. 3. AFM image of the 150-s sample grown at 700 °C, i.e., just after the appearance of 3D spots in RHEED patterns. The pyramidal clusters have completely disappeared. The surface is now characterized by two new kinds of islands of different sizes, each of them exhibiting a dome shape with large angle facets. (b) Island size distribution.

a diameter of about 70 nm and a height of 2.5–4 nm. The larger islands (indicated by B) are 180–200 nm in diameter and 40–45 nm in height. The concentration of small islands ($\sim 1 \times 10^8 \text{ cm}^{-2}$) is three times smaller than that of larger islands ($\sim 3 \times 10^8 \text{ cm}^{-2}$). The shape of the small islands is irregular while large islands exhibit $\{111\}$ facets (the measured inclination angle is $\sim 54^\circ$). The absence of pyramidal islands detected by AFM at this growth stage is therefore in agreement with the above PL results. The fact that the pyramidal islands completely “disappear,” both from the optical and structural points of view, to the benefit of 3D MI’s indicates unambiguously that they are metastable and act as precursors for the formation of 3D MI’s. To our knowledge, it is the first time that the metastability of the intermediate islands is experimentally demonstrated. To clearly distinguish these

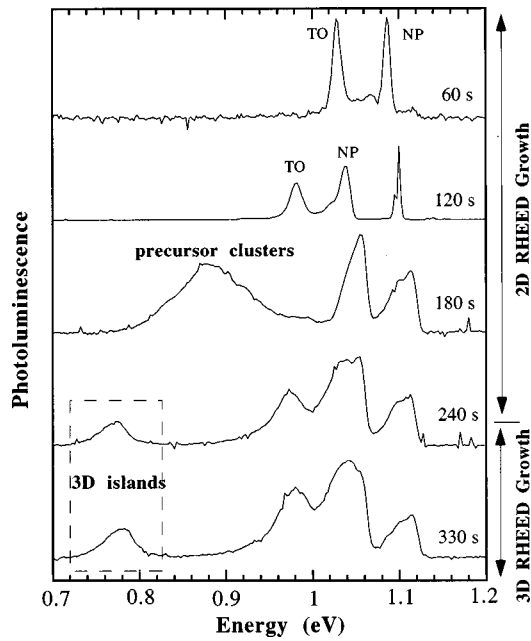


FIG. 4. 5-K PL spectra illustrating three distinct stages of Ge growth at 550 °C when increasing the deposition time: (i) the growth of the entirely pseudomorphic wetting layers up to $t_g = 120$ s; (ii) the formation of the intermediate and metastable precursor clusters between 2D layers and 3D MI's at $t_g = 180$ s; (iii) the formation of 3D macroscopic islands for $t_g \geq 240$ s. Note that the asymmetric PL bands around 1050 and 1115 meV are associated with a contamination of the Si cap layer.

intermediate islands from 3D MI's, we shall refer to them as "precursor clusters." It is worth noting that the 3D PL peak observed at 890 meV originates from the smaller 3D islands (A). Islands of ~ 200 nm in diameter (B) should give PL signals at an energy lower than 700 meV, which is beyond the Ge photodetector cutoff. Therefore, the relatively weak PL intensity observed at ~ 890 meV can be explained by a low concentration of islands (A). We also note that with a further increase of the deposition time, the surface became more inhomogeneous as a consequence of the formation of islands of multimodal size distributions.

Let us now consider the Ge growth at 550 °C. The evolution of the PL spectra illustrating different stages of Ge growth with increasing deposition time is shown in Fig. 4. Similar to the growth at 700 °C, three distinct stages are clearly identified: (i) the growth of entirely pseudomorphic wetting layers up to $t_g \sim 120$ s; (ii) the formation of metastable precursor clusters at $t_g \sim 180$ s, intermediate between 2D layers and 3D MI's; (iii) the formation of 3D macroscopic islands for $t_g \geq 240$ s. AFM measurements reveal that the intermediate clusters have *the same density and the same pyramidal shape* as those observed at 700 °C. Their base is 40–55 nm wide and their height is around 2 nm, which is consistent with a lower energy of the related PL band. The existence of an intermediate phase between 2D layers and 3D macroscopic islands is again established. It is also observed before the 2D-3D growth mode transition and exhibits a similar broadening. The main difference between the two growth temperatures concerns the energy position of the 3D MI's in PL, which is now located at 780 meV instead of 890 meV for samples grown at 700 °C. This indicates that

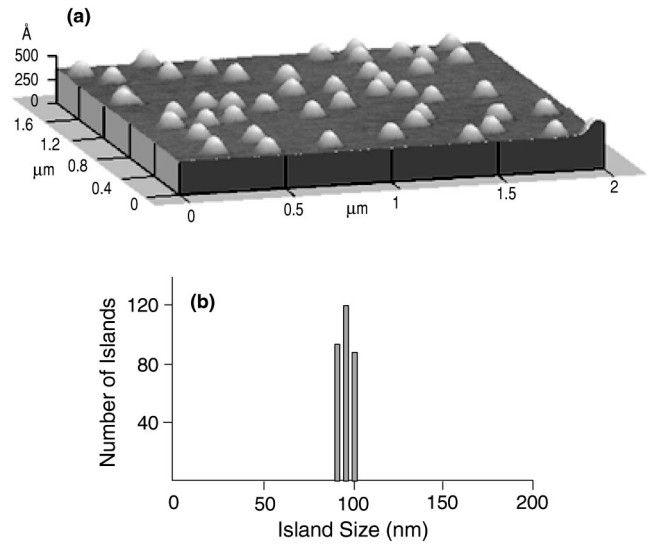


FIG. 5. A three-dimensional AFM image of a sample taken just after the 2D-3D transition at 550 °C ($t_g = 240$ s). The precursor clusters have completely disappeared. The surface exhibits islands which are highly uniform both in *size* and *height*, in contrast to the inhomogeneous surface observed at 700 °C (Fig. 3). (b) Island size distribution.

the corresponding 3D islands have at 550 °C larger sizes than at 700 °C. In contrast, the energy position of this PL peak does not significantly change for growth times longer than 240 s, a situation that is similar to that observed at 700 °C. The full width at half maximum of this peak is about 30–40 meV and the PL is observed up to room temperature.

Figure 5 shows a 3D AFM image of a sample taken just after the 2D-3D transition at 550 °C ($t_g = 240$ s). The size distribution is presented in Fig. 5(b). It can be clearly seen that the precursor clusters have completely disappeared. A spectacular result is that the surface now exhibits islands that are highly uniform both in size and height, in contrast to the inhomogeneous surface observed at 700 °C (Fig. 3). The average diameter of the islands is 95 nm with a relative deviation less than 5%. Their height is about 14 nm. The areal density of islands is about 2×10^9 cm $^{-2}$. Note that the islands have now {113} facets instead of {111} facets observed at 700 °C. What is also spectacular is the behavior observed with a further increase of the deposition time. The islands reach a nearly equilibrium configuration and two successive growth stages, named early and late growth, occur.¹⁹ Increasing t_g from 240 to ≤ 330 s only results in an increase of the island density, but not in changes in the island diameter and height. When the island density reaches an equilibrium value of $\sim 1 \times 10^{10}$ cm $^{-2}$, coalescence starts. Figure 6 shows an AFM image of a surface for $t_g = 330$ s, which illustrates the beginning of the coalescence process. We emphasize that the small islands have the same dimensions as those observed at the earliest stage of the 3D island growth ($t_g = 240$ s), and that they remain stable during the whole coalescence process.

The structural and optical results above have clearly defined three main stages of Ge/Si growth: 2D layer growth, formation of precursor clusters, and then 3D macroscopic islands. Of particular interest is the demonstration of an intermediate and metastable phase between 2D layers and 3D

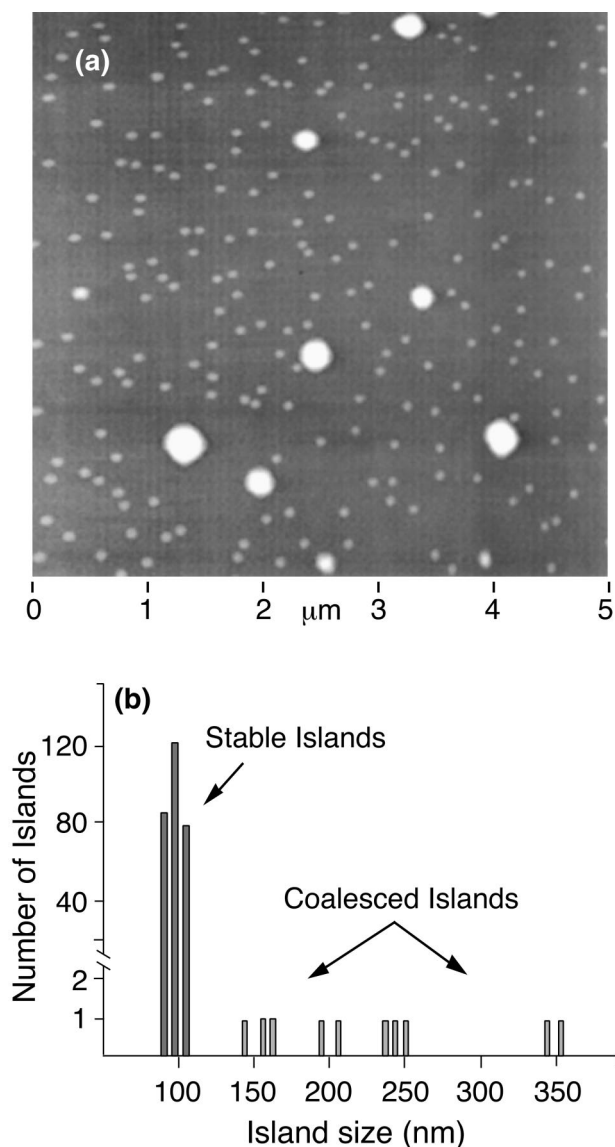


FIG. 6. An AFM image of a sample grown at 550 °C ($t_g = 330$ s), which illustrates the beginning of the coalescence process, giving to a multimodal size distribution. We note that the small islands have the same dimensions as those observed at the earliest stage of 3D island growth (Fig. 5). (b) A histogram of island size distributions.

macroscopic islands. This phase is found to appear just before the 2D-3D growth mode transition detected by RHEED. This phase exhibits a large three-dimensional confinement, and in the presence of this phase the PL of the wetting layer is quenched. The fact that almost the same clusters have been observed over the whole temperature range under investigation (550–700 °C) indicates that their formation are not thermally activated. Their appearance then seems to be intrinsic of the early stage of the strain relaxation processes in the Ge/Si system. It is worth noting that the small height and, in particular, the very low density of precursor clusters allows us to explain the streaky RHEED patterns observed at this growth stage. Indeed, since the mean distance between is-

lands is about 1–2 μm, which is much larger than the coherence length of RHEED (~ 30 –50 nm),^{13,20} the presence of these islands can be considered as a limitation of the long-range order of the surface. It manifests only in the quality of diffraction patterns, i.e., in increasing the intensity or/and in broadening the diffracted streaks. The growth behavior of the Si cap layers at this growth stage is, in contrast, not presently understood. A plausible explanation is that the Ge surface is morphologically unstable due to the presence of inhomogeneous strain fields just before the 2D-3D transition. The *island growth* for the first Si layers can be then explained by an asymmetric diffusion of Si adatoms in the presence of surface strain fields, a mechanism similar to that leading to the vertical self-organization in multilayer-array growth.²¹ After some Si islands have been formed, smoothing takes place as what happens on a Ge surface covered with 3D islands.

On the other hand, the formation of 3D macroscopic islands is found to be kinetically controlled. Two kinetic pathways are clearly identified vs growth temperature. At 550 °C, two growth stages (early and late growth) successively occur when the deposition time is increased. In the early stage, when t_g is between 240 and ≤ 330 s, the capture of atoms from the supersaturated adatoms only contributes to the increase of the island density. This suggests that the islands observed at this stage are stable. The coalescence at $t_g \sim 330$ s can be explained as follows. Existing islands are sufficiently dense so that incoming Ge adatoms can reach them without meeting another free adatom. The formation of new island is less than probable implying that the late growth regime starts. When the growth temperature increases, the surface diffusion coefficient of adatoms becomes larger and the coalescence process is expected to occur earlier. The broad size distributions of islands observed at 700 °C can be attributed to the high mobility of incoming adatoms or/and existing islands, which favors the coalescence process to take place even at the early growth stage. This might explain the formation of high-density and large islands (islands B, Fig. 3) at the early growth stage.

In conclusion, we have established a relatively coherent picture of the Ge/Si islanding growth in a UHV-CVD system. We have given evidence of the existence of an intermediate phase between 2D layers and 3D macroscopic islands. We have demonstrated, to our knowledge for the first time, that this phase is metastable against the formation of 3D macroscopic islands. Our results suggest that the 2D-3D transition is not so spontaneous as currently believed. The formation of 3D macroscopic islands is shown to be kinetically controlled. The surface mobility of adatoms appears to be the key parameter that determines the island size distributions. Uniform islands can be formed only at the early growth stage and at a low growth temperature. We have also confirmed that *in situ* RHEED is a powerful technique for probing the evolution of the film morphology in an UHV-CVD system.²²

This work has been supported by CNET under Convention No. 981B044.

- ¹See, for example, P. M. Petroff and G. Mederios-Riberio, *Mater. Res. Bull.* **21**, 50 (1996), and references therein.
- ²D. J. Eaglesham and M. Cerullo, *Phys. Rev. Lett.* **64**, 1943 (1990).
- ³J. M. Moison, F. Houzay, F. Barthe, L. Leprince, E. André, and O. Vatel, *Appl. Phys. Lett.* **64**, 196 (1994); D. Leonard, K. Pond, and P. M. Petroff, *Phys. Rev. B* **50**, 11 687 (1994).
- ⁴P. Schittenhelm, G. Abstreiter, A. Darhuber, G. Bauer, P. Werner, and A. Kosogov, *Thin Solid Films* **294**, 291 (1997).
- ⁵L. Vescan, W. Jäger, C. Dieker, K. Schmidt, A. Hartmann, and H. Lüth, in *Mechanisms of Heteroepitaxial Growth*, edited by M. F. Chisholm, R. Hull, L. J. Schowalter, and B. J. Garrison, MRS Symposia Proceedings No. 263 (Materials Research Society, Pittsburgh, PA, 1992), p. 23); G. Capellini, L. Di Gaspare, F. Evangelisti, and E. Palange, *Appl. Phys. Lett.* **70**, 493 (1997).
- ⁶Y.-W. Mo, D. E. Savage, B. S. Swartzentruber, and M. G. Lagally, *Phys. Rev. Lett.* **65**, 1020 (1990).
- ⁷M. Tomitori, K. Watanabe, M. Kobayashi, and O. Nishikawa, *Appl. Surf. Sci.* **76/77**, 322 (1994).
- ⁸I. Goldfarb, P. T. Hayden, J. H. G. Owen, and G. A. D. Briggs, *Phys. Rev. Lett.* **78**, 3959 (1997); *Phys. Rev. B* **56**, 10 459 (1997).
- ⁹See, for example, D. W. Greve, *Mater. Sci. Eng., B* **18**, 22 (1993), and references therein.
- ¹⁰M. Goryll, L. Vescan, K. Schmidt, S. Mesters, H. Lüth, and K. Szot, *Appl. Phys. Lett.* **71**, 410 (1997).
- ¹¹T. I. Kamins, E. C. Carr, R. S. Williams, and S. J. Rosner, *J. Appl. Phys.* **81**, 211 (1997).
- ¹²V. Le Thanh, D. Bouchier, and D. Débarre, *Phys. Rev. B* **56**, 10 505 (1997).
- ¹³M. G. Lagally and D. E. Savage, *Mater. Res. Bull.* **18**, 24 (1993).
- ¹⁴V. Le Thanh, *Thin Solid Films* **321**, 98 (1998).
- ¹⁵J. Weber and M. I. Alonso, *Phys. Rev. B* **40**, 5683 (1989).
- ¹⁶H. Sunamura, N. Usami, Y. Shiraki, and S. Fukatsu, *Appl. Phys. Lett.* **66**, 3024 (1995).
- ¹⁷P. Schittenhelm, M. Gail, J. Brunner, J. F. Nützel, and G. Abstreiter, *Appl. Phys. Lett.* **67**, 1292 (1995).
- ¹⁸F. M. Ross, J. Tersoff, and R. M. Tromp, *Phys. Rev. Lett.* **80**, 984 (1998).
- ¹⁹M. Zinke-Allmang, L. C. Feldman, and M. H. Grabow, *Surf. Sci. Rep.* **16**, 377 (1992).
- ²⁰V. Le Thanh, M. Eddrief, C. Sébenne, A. Sacuto, and M. Balkanski, *J. Cryst. Growth* **135**, 1 (1994).
- ²¹Q. Xie, A. Madhukar, P. Chen, and N. P. Kobayashi, *Phys. Rev. Lett.* **75**, 2542 (1995); C. Teichert, M. G. Lagally, L. J. Petricolas, J. C. Bean, and J. Tersoff, *Phys. Rev. B* **53**, 16 334 (1996).
- ²²V. Le Thanh, V. Aubry-Fortuna, Y. Zheng, D. Bouchier, C. Guedj, and G. Hincelin, *Thin Solid Films* **294**, 59 (1997).